AIAA-2001-3322

A Hall Thruster Performance Model Incorporating the Effects of a Multiply-Charged Plasma

Richard R. Hofer
QSS Group, Inc.
Cleveland, OH

Robert S. Jankovsky
NASA Glenn Research Center
Cleveland, OH

37th AIAA/ASME/SAE/ASEE
Joint Propulsion Conference & Exhibit
8-11 July 2001
Salt Lake City, Utah

A Hall Thruster Performance Model Incorporating the Effects of a Multiply-Charged Plasma

Richard R. Hofer[§]
QSS Group, Inc.
Cleveland, OH 44135 USA

Robert S. Jankovsky[§]
NASA Glenn Research Center
Cleveland, OH 44135 USA

Abstract

A Hall thruster performance model that predicts anode specific impulse, anode efficiency, and thrust is discussed. The model is derived as a function of a voltage loss parameter, an electron loss parameter, and the charge state of the plasma. Experimental data from SPT and TAL type thrusters up to discharge powers of 21.6 kW are used to determine the best fit for model parameters. General values for the model parameters are found, applicable to high power thrusters and irrespective of thruster type. Performance of a 50 kW thruster is calculated for an anode specific impulse of 2500 seconds or a discharge current of 100 A.

Introduction

The Hall effect thruster (HET) is a plasma propulsion device that has found application on-board spacecraft for stationkeeping, orbit transfers, orbit raising, and is being considered for interplanetary missions.[1-5] The combination of high specific impulse (I_{sp}) and thrust-to-power ratio makes the Hall thruster uniquely qualified to fill such a varied array of missions. In the HET, shown schematically in Figure 1, ions are accelerated by an axial electric field established between a downstream cathode and an upstream anode. An *essentially* radial magnetic field is applied in an annular discharge chamber that impedes the motion of migrating electrons due to the crossed electric and magnetic fields creating an azimuthal closed electron drift, the Hall current. Propellant is injected at the anode and collisions in the closed drift region create ions that are then accelerated producing thrust.[6-7] Commercially developed Hall thrusters typically operate between 50–60% efficiency, achieving specific impulses between 1500–2500 seconds.[8-18] Operation below 1500 s generally results in intolerable decay in thruster efficiencies (<35% efficiency around 1200 s specific impulse).[10] Operation above 2500 s has not been demonstrated for extended periods of time in the literature, but it is widely believed that the lifetime of a high I_{sp} Hall thruster will be significantly less due to the production of multiply-charged ions resulting from the higher voltages encountered in the discharge chamber.

The NASA Hall thruster program is an integrated technology program addressing many propulsion requirements of NASA, DoD, and commercial customers.[19] The program is implemented at the NASA Glenn Research Center (GRC) by the Power and On-Board Propulsion Division, On-Board Propulsion Branch. As part of this program, investigations of the physical limits of HETs with the goal of extending the operational envelope are being conducted. One way of gaining insight into these limits is through the development of an analytical model that captures the relevant trends of the physical processes in question. To this end, a performance model was developed at NASA GRC. The model predicts thrust, anode specific impulse, and anode efficiency while incorporating the effects of a multiply-charged plasma. Free parameters in the model are found that best fit the experimental data from existing high power (>3 kW) HETs. This approach decreases the uncertainty when predicting the performance quantities for HETs with power levels approaching 50 kW. Predicting the performance at 50 kW is of interest due to current NASA efforts to design and fabricate thrusters at this power level.

Other researchers have developed methods for predicting the performance trends of an HET. These range from simple correlations between theoretically obtainable values and experimental results,[20] to more complex models derived from dimensionless scaling.[21-22] More recently, researchers at Space Power Inc. (now Pratt & Whitney)[16] and the Busek Co.[17] have almost simultaneously developed essentially identical two parameter models that predict the performance quantities. These efforts have demonstrated the

[§]Research Scientist, Member AIAA

successful application of the model to thrusters from the same manufacturer. Values used in the models for the parameters have also roughly compared for power levels above 3 kW. The model presented here builds on the work of previous researchers by adding the extra parameters associated with a multiply-charged plasma, and determining model parameters applicable to a range of high power HETs.

Model Equations

The goal of the model is to derive equations for the performance quantities thrust, anode specific impulse, and anode efficiency. The derivation begins with the standard definitions in Equations 1-3.

$$T = \dot{m}_a v_e \tag{1}$$

$$I_{sp} = \frac{T}{\dot{m}_a g} \tag{2}$$

$$h = \frac{P_{Jet}}{P_D} = \frac{\frac{1}{2} T v_e}{I_D V_D} = \frac{T^2}{2\dot{m}_a P_D} \tag{3}$$

Equations 1-3 neglect cathode flow rate, magnet power, power processing unit (PPU) efficiency, and other parasitic losses that may exist in a propulsion system. This approach is mandated by the variability in design approaches of the various thrusters, i.e. some thrusters have more optimized cathodes, more efficient magnetic circuits, etc. For thrusters with discharge powers larger than 1 kW, typically cathode flow rate is 4-8% of the total flow rate,[8,9,14,16] magnet power is 1-4% of the total input power,[9] and PPU efficiencies are 90-95%.[23,24]

Any differences between the two major types of HETs were neglected in the derivation of the performance equations. These are the stationary plasma thruster (SPT), which is characterized primarily by a ceramic discharge chamber, and the anode layer thruster (TAL), which is characterized primarily by a metallic discharge chamber. Although differences do exist between SPTs and TALs, their performance quantities are equivalent for thrusters of the same discharge voltage and current.[13]

Singly-Charged Plasma Model

In an ideal thruster, the discharge voltage is the applied potential through which an ion would be accelerated. However, cathodes typically float between 10-30 V below spacecraft ground[9,13-16] and the plasma potential around one meter downstream of the exit will still be 5-10 V above spacecraft ground.[25-26] Both of these effects lower the maximum accelerating potential that an ion can be accelerated through. Further, because ions are created in the discharge chamber at different axial locations, the plasma exhaust from HETs has a spread in ion velocities,[27-28] as each ion is accelerated by the voltage drop corresponding to where it was created. The average exit velocity for the thruster as a whole is also affected by the charge state of each ion and the ion beam divergence. To take into account all of these considerations, an average accelerating voltage, V_A, and a voltage loss parameter, ΔV, are defined. The sum of these quantities is simply the discharge voltage, given by Equation 4.

$$V_D \equiv V_A + \Delta V \tag{4}$$

In the HET, ions are accelerated electrostatically.[7] The average exhaust velocity can then be found through energy conservation, assuming the initial neutral velocity of the propellant is negligible and that the plasma consists solely of singly charged xenon ions.

$$\frac{1}{2} m_{xe} v_e^2 = e V_A \tag{5}$$

Solving for the average exit velocity and substituting Equation 4, a relationship between the exhaust velocity, the discharge voltage, and the voltage loss parameter is found.

$$v_e = \sqrt{\frac{2eV_A}{m_{xe}}} = \sqrt{\frac{2e(V_D - \Delta V)}{m_{xe}}} \tag{6}$$

It will also be convenient to define the voltage loss parameter defect velocity.

$$\Delta u \equiv \sqrt{\frac{2e\Delta V}{m_{xe}}} \tag{7}$$

The discharge current in an HET is the sum of the ion current and electron current.

$$I_D = I_B + I_e \tag{8}$$

If the electron loss parameter is defined in Equation 9 as the ratio between the electron current and the discharge current, an expression for the ion current can be found by substitution into Equation 8.

$$i \equiv \frac{I_e}{I_D} \tag{9}$$

$$I_B = (1 - i) I_D \tag{10}$$

The electron loss parameter must place an upper limit on the efficiency, since it quantifies how much of the discharge current is electron current. HETs operating above 200 V typically exhibit electron currents that are 20-30% of the discharge current.[7] Assuming that this ratio is immutable and fundamental to HET operation, efficiencies should plateau at 70-80%.

From mass conservation, the anode flow rate must be the sum of the mass flow equivalent ion current and "neutral current"[¥].

$$\dot{m}_a = \frac{m_{xe}}{e}\left(I_B + I_n\right) \tag{11}$$

The neutral current is neglected since the ion velocity is typically two orders of magnitude greater than the neutral velocity. This is supported by measurements of the ratio of ion current to the neutral current in SPTs that show this value may be as high as unity.[7]

$$I_B >> I_n \text{ since } v_e >> v_n \tag{12}$$

$$\dot{m}_a \cong \frac{m_{xe}}{e} I_B \cong \frac{m_{xe}}{e}(1-i)I_D \tag{13}$$

With the above, it is possible to derive equations for the performance quantities, which will be denoted by a plus sign to signify that they assume a plasma of singly-charged ions. Thrust is obtained by substituting Equations 6 and 13 into Equation 1.

$$\begin{aligned} T^+ &= \dot{m}_a v_e = (1-i)I_D\sqrt{\frac{2m_{xe}}{e}(V_D - \Delta V)} \\ &= (1-i)\frac{P_D}{V_D}\sqrt{\frac{2m_{xe}}{e}(V_D - \Delta V)} \end{aligned} \tag{14}$$

Equation 14 provides a way to obtain either constant current or constant power curves as a function of the discharge voltage and the loss parameters. Anode I_{sp} is now found by substituting Equations 1 and 6 into Equation 2.

$$I_{sp}^+ = \frac{T^+}{\dot{m}_a g} = \frac{\dot{m}_a v_e}{\dot{m}_a g} = \frac{1}{g}\sqrt{\frac{2e(V_D - \Delta V)}{m_{xe}}} \tag{15}$$

The I_{sp} is only a function of the discharge voltage and voltage loss parameter. This will make it possible to independently fit the voltage loss parameter by considering plots of I_{sp} versus V_D. Now solve Equation 15 for the inverse of the discharge voltage, and an alternate form of the thrust as a function of I_{sp} can be derived.

$$\frac{1}{V_D} = \frac{2e}{m_{xe}}\frac{1}{\left(I_{sp}^+ g\right)^2 + (\Delta u)^2} \tag{16}$$

$$\begin{aligned} T^+ &= \dot{m}_a v_e = \left(\frac{m_{xe}}{e}(1-i)I_D\right) g I_{sp}^+ \\ &= \left(\frac{m_{xe}}{e}(1-i)\frac{P_D}{V_D}\right) g I_{sp}^+ \end{aligned} \tag{17}$$

Now substitute Equation 16 and simplify.

$$\begin{aligned} T^+ &= \frac{m_{xe}}{e}(1-i)P_D g I_{sp}^+ \frac{2e}{m_{xe}}\frac{1}{\left(I_{sp}^+ g\right)^2 + (\Delta u)^2}\frac{\left(I_{sp}^+ g\right)^2}{\left(I_{sp}^+ g\right)^2} \\ &= \frac{2P_D}{g I_{sp}^+}\frac{(1-i)}{1 + \left(\frac{\Delta u}{g I_{sp}^+}\right)^2} \end{aligned} \tag{18}$$

In the final form of Equation 18 maximum thrust occurs at the I_{sp} corresponding to the defect velocity. That is, maximum thrust is obtained when the condition in Equation 19 is met.

$$\text{For maximum thrust, } \Delta u = g I_{sp}^+ \tag{19}$$

Lastly, consider the efficiency. Substitution of Equation 6 and the constant current form of Equation 14 yields the following.

$$\begin{aligned} h^+ &= \frac{T^+ v_e}{2 I_D V_D} \\ &= \frac{(1-i)I_D}{2 I_D V_D}\sqrt{\frac{2m_{xe}}{e}(V_D - \Delta V)}\sqrt{\frac{2e(V_D - \Delta V)}{m_{xe}}} \\ &= \left(1 - \frac{\Delta V}{V_D}\right)(1-i) \end{aligned} \tag{20}$$

An alternate form of the efficiency as a function of I_{sp} is obtained by substituting in Equation 18.

$$h^+ = \frac{2P_D}{g I_{sp}^+}\frac{(1-i)}{1 + \left(\frac{\Delta u}{g I_{sp}^+}\right)^2}\frac{g I_{sp}^+}{2P_D} = \frac{(1-i)}{1 + \left(\frac{\Delta u}{g I_{sp}}\right)^2} \tag{21}$$

In Equation 20, the efficiency is simply a function of the discharge voltage and the loss parameters. This makes it possible to determine a suitable value for the electron loss parameter once the voltage loss parameter has been determined using the I_{sp} given in Equation 15. Further, Equation 20 shows how the efficiency asymptotically approaches the value of (1-i) at high discharge voltages.

[¥] The definition of a neutral current is simply a matter of convenience. The neutral current assumes a positive charge of unity, a thermal velocity corresponding to the anode temperature (~1000 K), and the number density corresponding to the difference between the anode flow number density and the ion density.

Multiply-Charged Plasma Model

The equations for thrust, I_{sp}, and efficiency thus far all assume a plasma consisting of singly-charged ions. This description is not always adequate to describe HET performance behavior, especially at high mass flow rates and high voltages. One possible explanation for this behavior is the effect of a multiply-charged plasma on thruster performance. In order to show how this changes the performance, several new definitions are needed. The following is a generalization of the work presented by Vahrenkamp[29] to explain multiply-charged effects in ion thrusters. First, consider an ion beam consisting of n charged species (e.g. Xe^{+}, Xe^{2+}, Xe^{3+}, …, Xe^{n+}). Define the fraction of species i as the ratio of the species density to the beam density.

$$z_i = \frac{n_i}{n_B} = \text{species fraction} \tag{22}$$

The current of the i^{th} species, assuming an accelerating voltage of V_A will be taken as the following.

$$\begin{aligned} I_i &= An_i q_i v_{e,i} = An_i eZ_i \sqrt{\frac{2eZ_i V_A}{m_{xe}}} \\ &= An_i Z_i^{3/2} e^{3/2} \sqrt{\frac{2V_A}{m_{xe}}} \end{aligned} \tag{23}$$

In the above it is assumed that each species is accelerated through the same accelerating voltage, V_A. It seems more likely that the higher charge states will be born at axial locations further downstream of the next lowest, but such considerations will be neglected in lieu of adding yet another level of complexity to the model.

The beam current is the sum of each of the currents carried by species i. Summations below are assumed to occur over each species i from 1 to n.

$$\begin{aligned} I_B &= \sum I_i = A\sum n_i q_i v_{e,i} \\ &= Ae^{3/2} \sqrt{\frac{2V_A}{m_{xe}}} \sum n_i Z_i^{3/2} \end{aligned} \tag{24}$$

Making use of Equations 22-24 the current fraction of species i is the ratio of species current to the beam current.

$$\Omega_i = \frac{I_i}{I_B} = \frac{z_i Z_i^{3/2}}{\sum z_i Z_i^{3/2}} \tag{25}$$

The motivation for using Equation 25 stems from experimental results using energy diagnostics that typically yields species fraction information.[27-28] Equation 25 will allow for conversion of those data in the model, where species current fractions are more convenient.

Equations 22-25 make it possible to modify the performance model for the effects of a multiply-charged plasma. First, Equation 6 is modified to account for the average exit velocity of the i^{th} species as follows.

$$v_{e,i} = \sqrt{\frac{2e(V_D - \Delta V)}{m_{xe}}} \sqrt{Z_i} \tag{26}$$

The beam current relationship, Equation 10, remains unchanged. Equation 27 give the mass flow rate of each species, and the anode mass flow rate is the sum of each species flow rate given by Equation 28. The final form for the anode mass flow rate is obtained by substituting Equations 10 and 25.

$$\dot{m}_i \cong \frac{m_{xe}}{e} \frac{I_i}{Z_i} \tag{27}$$

$$\dot{m}_a \cong \sum \dot{m}_i = \frac{m_{xe}}{e}(1-i) I_D \sum \frac{\Omega_i}{Z_i} \tag{28}$$

The quantity given by the summation in Equation 28 is always less than one, so the mass flow rate of a multiply-charged plasma (for the same beam current), is always less than that of a singly-charged plasma.

The thrust of a multiply-charged plasma is given by the sum of the thrust contribution each ion species imparts to the spacecraft. The final form below is derived by substituting Equations 10, 25, 26, and 27.

$$\begin{aligned} T &= \sum \dot{m}_i v_{e,i} = \sqrt{\frac{2e(V_D - \Delta V)}{m_{xe}}} \frac{m_{xe}}{e} \sum \frac{I_i}{Z_i} \sqrt{Z_i} \frac{I_B}{I_B} \\ &= (1-i) I_D \sqrt{\frac{2m_{xe}(V_D - \Delta V)}{e}} \sum \frac{\Omega_i}{\sqrt{Z_i}} \\ &= (1-i) \frac{P_D}{V_D} \sqrt{\frac{2m_{xe}(V_D - \Delta V)}{e}} \sum \frac{\Omega_i}{\sqrt{Z_i}} \\ &= T^{+} \sum \frac{\Omega_i}{\sqrt{Z_i}} \end{aligned} \tag{29}$$

In the final form of Equation 29 above, the thrust of a multiply-charged plasma is simply the singly-charged thrust multiplied by the value of the summation. The quantity given by the summation is always less than unity, which implies that the thrust of a multiply-charged plasma (for the same beam current), is always less than that of a singly-charged plasma. It is important to emphasize that a comparison between a singly- and multiply-charged plasma for the same beam current is being considered. If the comparison is

between equivalent mass flow rates, then the thrust of a multiply-charged plasma would be greater than the singly-charged version because the average exit velocity of a multiply-charged plasma would be greater.

Considering I_{sp} now, the mass flow rates do not cancel as they did in Equation 15 because of the summations. The derivation below makes use of Equations 10 and 29.

$$I_{sp} = \frac{T}{\dot{m}_a g} = \frac{\sum \dot{m}_i v_{e,i}}{g \sum \dot{m}_i}$$

$$= \frac{(1-i) I_D}{g} \sqrt{\frac{2 m_{xe} (V_D - \Delta V)}{e}} \frac{\sum \frac{\Omega_i}{\sqrt{Z_i}}}{\frac{m_{xe}}{e}(1-i) I_D \sum \frac{\Omega_i}{Z_i}} \quad \textbf{(30)}$$

$$= \frac{1}{g} \sqrt{\frac{2e(V_D - \Delta V)}{m_{xe}}} \frac{\sum \frac{\Omega_i}{\sqrt{Z_i}}}{\sum \frac{\Omega_i}{Z_i}} = I_{sp}^{+} \frac{\sum \frac{\Omega_i}{\sqrt{Z_i}}}{\sum \frac{\Omega_i}{Z_i}}$$

Similarly to the thrust, the multiply-charged version of the I_{sp} is the singly-charged value multiplied by the value of the summation given above. Because the quantity given by the summation is always greater than one, the anode I_{sp} of a multiply-charged plasma (for the same beam current), is always greater than that of a singly-charged plasma.

Finally, efficiency is derived starting with Equation 3 and substituting Equations 28-29.

$$h = \frac{T^2}{2 \dot{m}_a P_D}$$

$$= \frac{\left((1-i) I_D \sqrt{\frac{2 m_{xe} (V_D - \Delta V)}{e}} \sum \frac{\Omega_i}{\sqrt{Z_i}} \right)^2}{2 \frac{m_{xe}}{e} (1-i) I_D \sum \frac{\Omega_i}{Z_i} P_D} \quad \textbf{(31)}$$

$$= \left(1 - \frac{\Delta V}{V_D}\right)(1-i) \frac{\left(\sum \Omega_i / \sqrt{Z_i} \right)^2}{\sum \Omega_i / Z_i} = h^{+} \frac{\left(\sum \Omega_i / \sqrt{Z_i} \right)^2}{\sum \Omega_i / Z_i}$$

Again, the multiply-charged version is the singly-charged value multiplied by the value of the summation given above. The summation in the final line of Equation 31 is always less than one, so the efficiency of a multiply-charged plasma (for the same beam current), is always less than that of a singly-charged plasma.

Fitting Model Parameters

As shown above, the singly-charged model for I_{sp} is a function of the voltage loss parameter while the efficiency is a function of both the voltage loss and electron loss parameters. This enables the singly-charged model parameters to be fit sequentially beginning with the I_{sp}, next the efficiency, and then the thrust is given based off the previous fits. For the multiply-charged model, species fraction data is taken directly from experiment. This is done because of the large number of free parameters introduced by a multiply-charged plasma. Borrowing from experiment essentially reduces all of the multiply-charged considerations to one lumped parameter. The loss parameters from the singly-charged model are used for the multiply-charged model as well. This is done based on the underlying assumption that the production of multiply-charged ions in the plasma will not change those physical processes in the thruster that determine the loss parameters. Lastly, the final values of the model parameters are determined based on the best fit to thrusters with discharge powers greater than 3 kW, with emphasis on matching data from the 10 kW T-220 and the TM-50 at a maximum power of 21.6 kW. This approach is taken so that extrapolation of the model to power levels of 50 kW can be done with greater confidence than if the model was tuned to low power thrusters. Data from thrusters as low as 0.66 kW will also be used to highlight that the model parameters used here are not generally applicable to low power thrusters.

Multiply-Charged Plasma Parameters

The multiply-charged model introduces several new quantities as shown in Equations 28-31. Instead of fitting the model to data using arbitrary values, experimental data is used to determine the necessary summations. Experiments by King[27] and Gulczinski[28] at the University of Michigan using a time-of-flight mass spectrometer are used and shown in Table 1. Both researchers obtained ion species fraction data using the instrument. This data can be readily converted into ion current fractions using Equation 25. King's data was taken 0.5 m downstream of an SPT-100 operating at 300 V and 4.5 A. Gulczinski's data is 0.75 m downstream from the University of Michigan 5 kW P5 laboratory Hall thruster operating at 300 V, 5.2 A. In the model, the average of the data is taken and used to compute ion current fractions. Although the ion species fractions have been shown to be a function of voltage and flow rate,[28] the multiply-charged model will neglect such considerations.

Voltage Loss Parameter

Figure 2 plots data from several thrusters[8-18] as I_{sp} versus discharge voltage. Curves labeled "theory" assume no voltage loss while the "model" curves are those predicted by the model. The voltage loss parameter was fit to 50 V for both models. The data

from the nominally 10 kW T-220 closely matches the singly-charged model over a large range of voltages. Data from the TM-50 operating at up to 21.6 kW begins to exceed the theoretical limit for a singly-charged plasma above 500 V, but closely matches the multiply-charged model over a large voltage range. Taken together, the figure demonstrates that both models capture the functional relationships.

Although the voltage loss parameter is tuned for high power thrusters in the figure, data from several low power thrusters are also shown. For example, to match the I_{sp} of the SPT-70 a voltage loss parameter of 134 V is needed for the singly-charged model. While the SPT-100 requires the parameter to be set to 103 V. Table 2 lists the performance of these two thrusters and the loss parameters necessary to match their performance quantities. The predicted thrust simply falls out once the loss parameters are determined and the agreement is excellent for these thrusters.

Electron Loss Parameter

Figure 3 plots efficiency versus discharge voltage for several thrusters and the singly- and multiply-charged models. The voltage loss parameter is 50 V and the electron loss parameter is fit to 0.26. Other low power thrusters are shown to highlight how the model parameters are fit for high power HETs. The T-220 data exceeds either model at voltages above 300 V, but is less than the models below 300 V. The TM-50 data finds better agreement, following the multiply-charged model the best. It is worth noting that experimentally determined efficiency data typically has an uncertainty of 3-5%, depending on the care with which the data is taken, so much of the data would still fall within the values predicted by the models. Regardless, a more likely explanation of the quality of the fit is that the electron loss parameter is a function of the discharge voltage. The well-known current-voltage characteristic of an HET illustrates why this may true. Kim[7] reports that the ion current in an SPT reaches some fraction of the discharge current at voltages above 120 V and then remains unchanged. However, the discharge current is still changing above 120 V indicating that the electron current is varying. Accounting for the dependence of the electron loss parameter with discharge voltage is beyond the scope of this work and will be neglected.

Predicting Thrust

With the loss parameters and the species fractions now set, the thrust can be calculated. Figure 4 plots thrust versus discharge voltage for several constant power and constant current curves. A subset of the thrusters from Figures 2 and 3 is shown for clarity. Shown are data from the T-140, the T-220, and the TM-50. At low power (3.4 kW) the singly-charged model follows the thruster data the best, at intermediate powers (10 kW) the thruster data falls in between the singly- and multiply-charged models, and at high power (21.6 kW) the multiply-charged model follows the thruster data the closest. Overall, the singly- and multiply-charged models are successfully bounding the data up to power levels of 21.6 kW.

High Power Predictions

With the model parameters determined, extrapolations of the model up to 50 kW and 100 A are calculated. Figure 5 plots thrust versus discharge voltage for various constant power and constant current curves. Both versions of the model are included in the figure, although multiply-charged effects are expected to dominate the performance at high power. Depending on the efficacy of the design, the different models should at least bound the performance. The intersection of 50 kW and 100 A curves is indicated as well, highlighting the performance of a 500 V thruster.

Table 3 presents the performance of a 50 kW thruster operating either at an I_{sp} of 2500 s or at a discharge current of 100 A. Either approach yields a thrust on the order of 2.5 N with efficiencies greater than 64%.

Conclusions

A performance model that includes the effects of a multiply-charged plasma has been developed. The voltage loss parameter was fit to 50 V, the electron loss parameter was fit to 0.26, and the species fraction data was taken from experiment. Whether the model is used for singly- or multiply-charged plasmas, the predictions bound the existing data for Hall thrusters that are in excess of 3 kW discharge power. Owing to the success of the model at powers of 3-21.6 kW, extrapolation to a power level of 50 kW to predict performance has been performed. The resulting calculation yields a thrust on the order of 2.5 N with efficiencies greater than 64%.

Nomenclature

A	= area, m^2
e	= electron charge, C
g	= gravitational acceleration, m/s^2
i	= electron loss parameter
I_B	= ion current, A
I_D	= discharge current, A
I_i	= current of the i^{th} ion species, A
I_e	= electron current, A
I_n	= neutral current, A
I_{sp}	= anode specific impulse, s
I_{sp}^+	= singly-charged plasma anode specific impulse, s
$\dot{m}_a$	= anode mass flow rate, mg/s
$\dot{m}_i$	= mass flow rate of the i^{th} ion species, mg/s
m_{xe}	= mass of a xenon atom, kg
n	= total number of ion species
n_B	= ion number density, m^{-3}
n_i	= number density of the i^{th} ion species, m^{-3}
P_{jet}	= jet power or beam power, W
P_D	= discharge power, W
q_i	= charge of the i^{th} ion species, eZ_i
T	= thrust, mN
T^+	= singly-charged plasma thrust, mN
V_A	= accelerating voltage, V
V_D	= discharge voltage, V
v_e	= average ion exit velocity, m/s
$v_{e,i}$	= average exit velocity of the i^{th} ion species, m/s
v_n	= average neutral velocity, m/s
Z_i	= ion charge state
Δu	= defect velocity, m/s
ΔV	= voltage loss parameter, V
η	= anode efficiency
η^+	= singly-charged plasma anode efficiency
Ω_i	= species current fraction of the i^{th} ion species
ζ_i	= species fraction of the i^{th} ion species

Acknowledgements

The authors would like to thank D. Manzella, P. Peterson, and V. Rawlin for their input and guidance in developing this model. Additionally, we would like to thank M. Domonkos for his comments in preparing this manuscript.

References

1. Oleson, S. R., "Electric Propulsion for Low Earth Orbit Communications Satellites," IEPC-97-102, 25th International Electric Propulsion Conference, Cleveland, OH, Aug 24-28, 1997.

2. Oleson, S. R., Myers, R. M., "Advanced Propulsion for Geostationary Orbit Insertion and North-South Station Keeping," Journal of Spacecraft and Rockets, Vol. 34, No. 1, pp. 22-28, Jan-Feb 1997.

3. Oleson, S. R., "Advanced On-Board Propulsion for RLV Launched Spacecraft," IEPC-99-185, 26th International Electric Propulsion Conference, Kitakyushu, Japan, October 17-21, 1999.

4. Gefert, L. P., Hack, K. J., "Options for the Human Exploration of Mars Using Solar Electric Propulsion," AIP Conference Proceedings, No. 458, pp. 1275-1280, STAIF-99, Nov 1999.

5. Oleson, S. R., Sankovic, J. M., "Advanced Hall Electric Propulsion for Future In-Space Transportation," NASA TM-2001-210676.

6. Kaufman, H. R., "Technology of Closed-Drift Thrusters," AIAA Journal, Vol. 23, No. 1, January, 1985, pp. 78-87.

7. Kim, V., "Main Physical Features and Processes Determining the Performance of Stationary Plasma Thrusters," Journal of Propulsion and Power, Vol. 14, No. 5, Sept-Oct, 1998, pp. 736-743.

8. Jacobson, D., Jankovsky R., "Performance Evaluation of a 50 kW Hall Thruster," AIAA-99-0457, 37th Aerospace Sciences Meeting and Exhibit, Reno, NV, Jan 11-14, 1999.

9. Jankovsky, R. S., McLean, C., McVey, J., "Preliminary Evaluation of a 10 kW Hall Thruster," AIAA-99-0456, 37th Aerospace Sciences Meeting and Exhibit, Reno, NV, Jan 11-14, 1999.

10. Kim, V., Kozlov, V., Lazurenko, A., Popov, G., Skrylnikov, A., Clauss, C., Day, M., Sankovic, J., "Development and Characterization of Small SPT," AIAA-98-3335, 34th Joint Propulsion Conference, Cleveland, OH, July 13-15, 1998.

11. Kim, V., Grdlichko, D., Kozlov, V., Lazurenko, A., Popov, G., Skrylnikov, A., Day, M., "SPT-115 Development and Characterization," AIAA-99-2568, 35th Joint Propulsion Conference, Los Angeles, CA, June 20-24, 1999.

12. King, D., Tilley, D, Aadland, R., Nottingham, K., Smith, R., Roberts, C., Hruby, V., Pote, B., Monheiser, J., "Development of the BPT Family of U.S.-Designed Hall Current Thrusters for Commercial LEO and GEO Applications," AIAA-98-3338, 34th Joint Propulsion Conference, Cleveland, OH, July 13-15, 1998.

13. Manzella, D. H., Sankovic, J. M., "Hall Thruster Ion Beam Characterization," AIAA-95-2927, 31st Joint Propulsion Conference, San Diego, CA, July 10-12, 1995.

14. Manzella, D., Hamley, J., Miller, J., Clauss, C., Kozubsky, K. Gnizdor, R., "Operational Characteristics of the SPT-140 Hall Thruster," AIAA-97-2919, 33rd Joint Propulsion Conference, Seattle, WA, July 6-9, 1997.

15. Mason, L.S., Jankovsky, R.S., Manzella, D.H., "1000 Hours of Testing on a 10 Kilowatt Hall Effect Thruster," AIAA-2001-3773, 37th Joint Propulsion Conference, Salt Lake City, UT, July 8-11, 2001.

16. McLean, C. H., McVey, J.B., Schappell, D.T., "Testing of a U.S.-Built HET System for Orbit Transfer Applications," AIAA-99-2574, 35th Joint Propulsion Conference, Los Angeles, CA, June 20-24, 1999.

17. Pote, B., Hruby, V., Monheiser, J., "Performance of an 8 kW Hall Thruster," IEPC-99-080, 26th International Electric Propulsion Conference, Kitakyushu, Japan, October 17-21, 1999.

18. Sankovic, J. M., Manzella, D. H., Osborn, M. F., "RHETT2/EPDM Development Testing," IEPC-97-102, 25th International Electric Propulsion Conference, Cleveland, OH, Aug 24-28, 1997.

19. Jankovsky, R. S., Jacobson, D. T., Mason, L. S., Rawlin, V. K., Mantenieks, M. A., Manzella, D. H., Hofer, R. R., Peterson, P. Y., "NASA's Hall Thruster Program," AIAA-2001-3888, 37th Joint Propulsion Conference, Salt Lake City, UT, July 8-11, 2001.

20. Grishin, S. D., Erofeev, V. S., Zharinov, A. V., Naumkin, V. P., Safronov, I. N., "Characteristics of a Two-Stage Ion Accelerator with an Anode Layer," Journal of Applied Mathematics and Technical Physics, No. 2, pp. 28-36, Mar-Apr 1978.

21. Bugrova, A. I., Maslennikov, N. A., Morozov, A. I., "Similarity Laws for the Global Properties of a Hall Accelerator," Soviet Physics: Technical Physics, Vol. 36, No. 6, pp. 612-615, 1991.

22. Domonkos, M. T., "Hall Thruster Scaling," Internal NASA Memorandum, Sept. 2000.

23. Skelly, P. T., Kay, R. J., "RHETT/EPDM Power Processing Unit," IEPC-97-104, 25th International Electric Propulsion Conference, Cleveland, OH, Aug 24-28, 1997.

24. Declercq, H., Bourguignon, E., Scalais, T., Digoin, J. J., "Power Processing Unit for Stationary Plasma Thruster," IEPC-99-059, 26th International Electric Propulsion Conference, Kitakyushu, Japan, October 17-21, 1999.

25. King, L. B., Gallimore, A. D., Marrese, C. M., "Transport-Property Measurements in the Plume of an SPT-100 Hall Thruster," Journal of Propulsion and Power, Vol. 14, No. 3, pp. 327-335, May-June 1998.

26. Keidar, M., Boyd, I. D., "Effect of a Magnetic Field on the Plasma Plume from Hall Thrusters," Journal of Applied Physics, Vol. 86, No. 9, Nov. 1, 1999.

27. King, L. B., Gallimore, A. D., "Mass Spectral Measurements in the Plume of an SPT-100 Hall Thruster," Journal of Propulsion and Power, Vol. 16, No. 6, Nov-Dec 2000, pp. 1086-1092.

28. Gulczinski, F. S., Gallimore, A.D., "Near-Field Ion Energy and Species Measurements of a 5-kW Hall Thruster," Journal of Propulsion and Power, Vol. 17, No. 2, Mar-Apr 2001, pp. 418-427.

29. Vahrenkamp, R. P., "Measurement of Double Charged Ions in the Beam of a 30-cm Mercury Bombardment Thruster," AIAA-73-1057, AIAA 10th Electric Propulsion Conference, Lake Tahoe, NV, Oct 31 – Nov 2, 1973.

30. King, L.B., "Transport-property and Mass Spectral Measurements in the Plasma Exhaust Plume of a Hall-effect Space Propulsion System," Ph.D. Dissertation, University of Michigan, 1998.

	Species Fractions			Species Current Fractions			Important Summations			
	Xe+	Xe2+	Xe3+	Xe+	Xe2+	Xe3+	$\sum \frac{\Omega_i}{Z_i}$	$\sum \frac{\Omega_i}{\sqrt{Z_i}}$	$\frac{\sum \Omega_i/\sqrt{Z_i}}{\sum \Omega_i/Z_i}$	$\frac{\left(\sum \Omega_i/\sqrt{Z_i}\right)^2}{\sum \Omega_i/Z_i}$
SPT-100, King	0.888	0.110	0.002	0.734	0.257	0.009	0.866	0.921	1.064	0.980
P5, Gulczinski	0.925	0.068	0.007	0.802	0.167	0.032	0.896	0.938	1.047	0.982
Average	**0.907**	**0.089**	**0.005**	**0.767**	**0.213**	**0.020**	**0.880**	**0.929**	**1.056**	**0.981**

Table 1 – Xenon ion species fraction data as reported by King[27] and Gulczinski[28] from time-of-flight mass spectroscopy measurements. Species current fractions are computed, as are several summations that are used in the multiply-charged performance model.

							Singly-Charged Model Predictions				
	Vd, V	Id, A	Anode Mass Flow, mg/s	Anode Isp, sec	Anode Efficiency	Thrust, mN	ΔV, V	i	Anode Isp, sec	Anode Efficiency	Thrust, mN
SPT-70	300	2.2	2.56	1593	0.47	40	134	0.15	1592	0.47	40
SPT-100	300	4.5	4.99	1734	0.53	85	103	0.19	1735	0.53	84

Table 2 - Performance data for the SPT-70 and SPT-100 with loss parameters that fit the singly-charged model to the performance data.

P_d = 50 kW, Anode I_{sp} = 2500 sec		
	Singly-Charged Model	Multiply-Charged Model
V_d, V	459	417
I_d, A	108.9	119.9
Anode Efficiency	0.66	0.64
Thrust, mN	2689	2605
Anode Mass Flow Rate, mg/s	109.7	120.6

P_d = 50 kW, I_d = 100 A		
	Singly-Charged Model	Multiply-Charged Model
V_d, V	500	500
Anode I_{sp}, sec	2622	2768
Anode Efficiency	0.67	0.65
Thrust, mN	2590	2406
Anode Mass Flow Rate, mg/s	100.7	88.6

Table 3 – Model predictions of a 50 kW Hall thruster for an anode I_{sp} of 2500 s or a discharge current of 100 A. Results from the singly- and multiply-charged models are presented, although the multiply-charged model is expected to be more accurate at high powers.

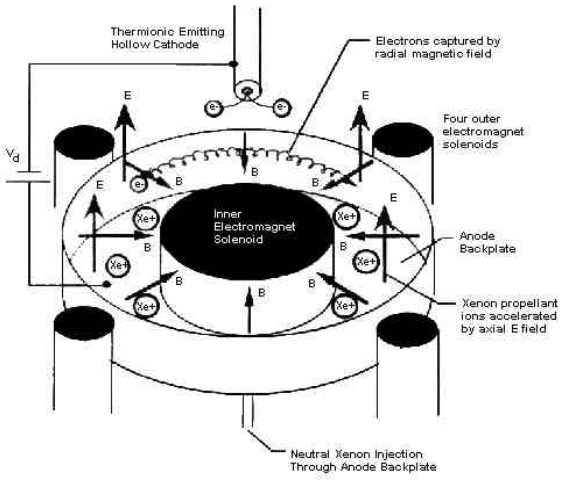

Figure 1 - The basic Hall thruster components showing the potential drop between the cathode and anode, the magnetic field circuit, and the closed electron drift induced by the crossed electric and magnetic fields. (Figure borrowed from Ref. 30).

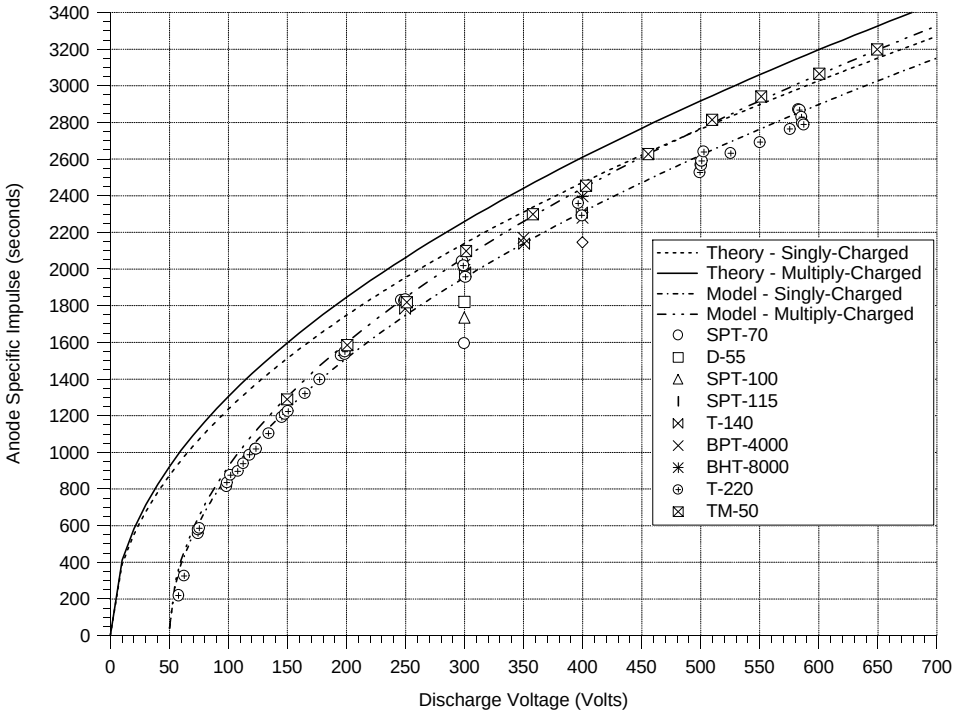

Figure 2 – Anode specific impulse versus discharge voltage. Theoretical and model curves are shown for a singly- or multiply-charged plasma. The voltage loss parameter is 50 V.

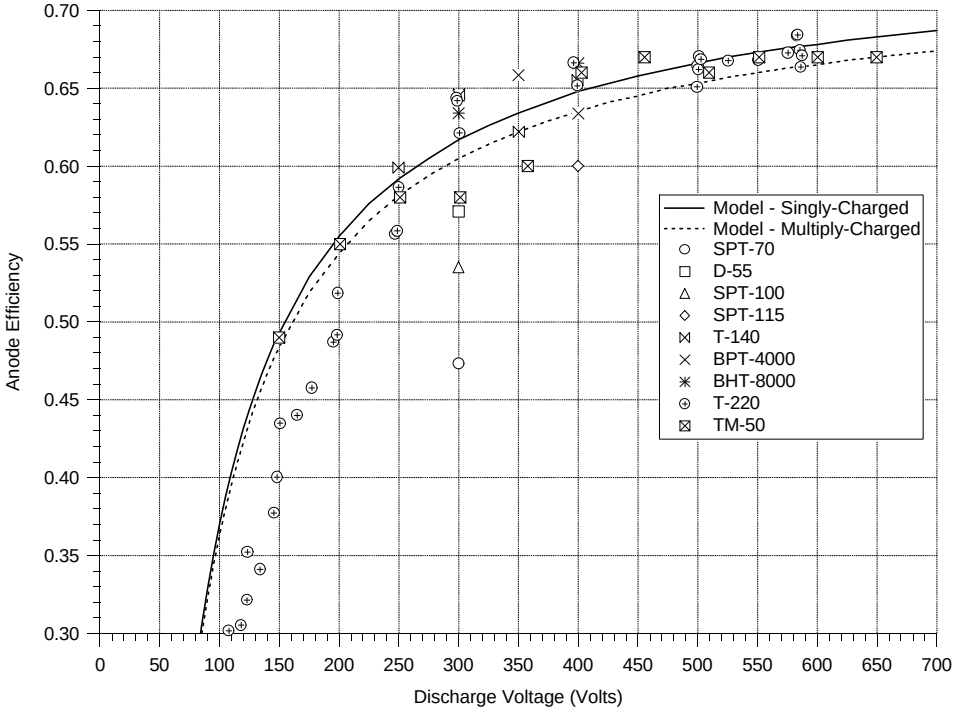

Figure 3 – Anode Efficiency versus discharge voltage. Model curves are shown for a singly- or multiply-charged plasma. The voltage loss parameter is 50 V, and the electron loss parameter is 0.26.

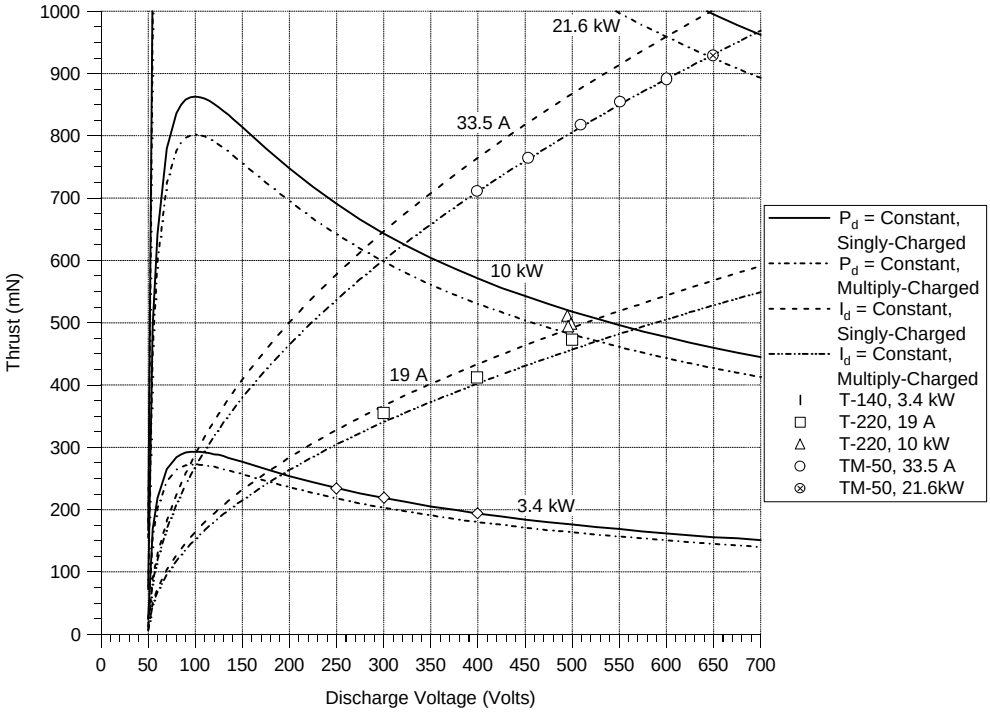

Figure 4 - Thrust versus discharge voltage. Constant power and constant current curves are shown for a singly- and multiply-charged plasma. The voltage loss parameter is 50 V, and the electron loss parameter is 0.26.

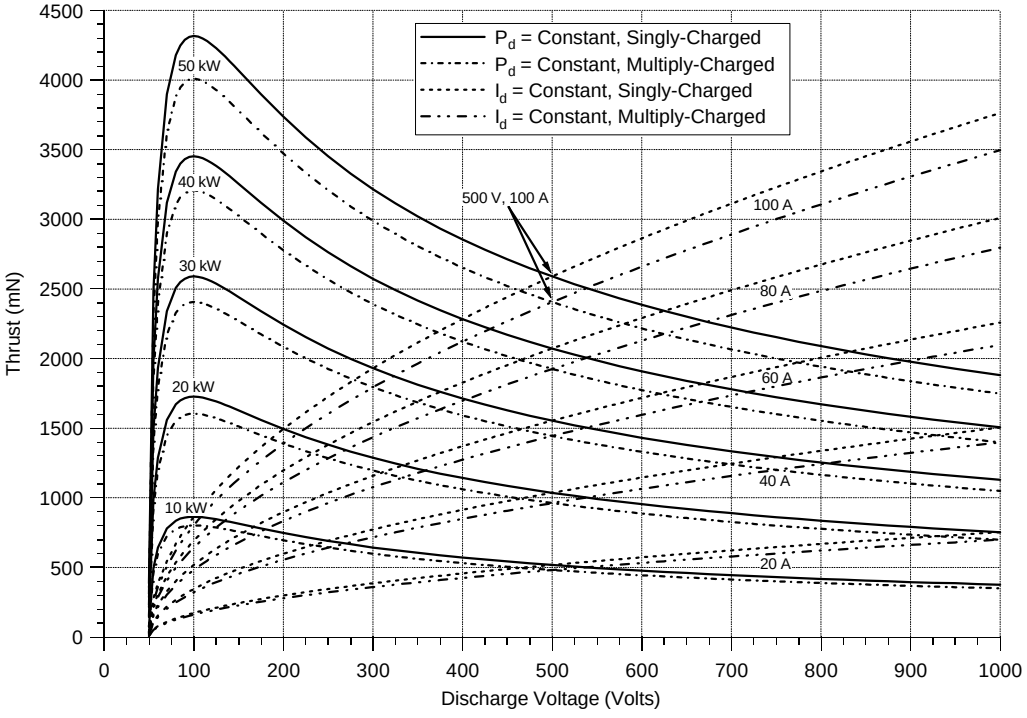

Figure 5 – Constant power and constant current curves for the singly- and multiply-charged performance models. The intersection of the 50 kW curve with the 100 A curve is indicated at 500 V.